Int. J. Electrochem. Sci., 17 **(2022)** Article Number: 22078, doi: 10.20964/2022.07.15

International Journal of
ELECTROCHEMICAL
SCIENCE
www.electrochemsci.org

Electroless Plating of Ni-P/Ni-Mo-P Duplex Coating on 16Mn Steel Weld Joint and its Corrosion Resistance in Natural Seawater

Chenqi Fu, Jinchun Sun, Ruijuan Guo, Lipeng Jiang, Shun Xu[*]

College of Engineering and Technology, Jilin Agricultural University, Changchun 130118, China
[*]E-mail: Edu_fu118@163.com

Received: 1 February 2022 / *Accepted:* 23 March 2022 / *Published:* 6 June 2022

A 16Mn steel plate is selected as the base substrate for welding, and a Ni-P/Ni-Mo-P duplex coating with Ni-P coating as the inner layer and Ni-Mo-P coating as the outer layer is prepared on the surface of weld joint by electroless plating. The appearance, surface morphology and composition of the substrate with and without Ni-P/Ni-Mo-P duplex coating were characterized, and the corrosion resistance of different coatings in seawater was compared and analyzed. The results show that the Ni-P single-layer coating, Ni-Mo-P single-layer coating and Ni-P/Ni-Mo-P duplex coating cover the weld joint completely showing a nodular morphology. The porosity of Ni-P/Ni-Mo-P duplex coating is only 1.2 spot/cm^2 for the best corrosion resistance, and its surface density is better than that of the Ni-P single-layer coating and Ni-Mo-P single-layer coating. Compared with the substrate, the corrosion current density of Ni-P/Ni-Mo-P duplex coating is reduced by nearly two orders of magnitude, and the protection efficiency reaches 98.5%, which can play a better role in corrosion protection and significantly improve corrosion resistance of 16Mn steel in natural seawater.

Keywords: Ni-P/Ni-Mo-P duplex coating; electroless plating; 16Mn steel weld joint; corrosion resistance

1. INTRODUCTION

16Mn steel has good welding property, excellent low-temperature impact toughness and a desirable mechanical property profile and is mainly applied to welded structures [1-3]. Due to a series of non-equilibrium physical and chemical processes that occur in the welding process, the composition and structure of the weld joint are not uniform. Defects such as incomplete penetration, incomplete fusion and pores are easily generated. In a seawater environment, chloride salts, sulfates and carbonates can cause localized corrosion of the weld joint, such as pitting corrosion, stress corrosion and galvanic corrosion, making them vulnerable to corrosion failure [4-8]. Therefore, it is necessary to

improve the corrosion resistance of the weld joint through surface treatment, which is crucial to ensure the stability and reliability of 16Mn steel welded structure.

Electroless plating is a commonly used surface treatment process for metal materials. It has the advantages of simple process flow, low cost, uniform and controllable coating thickness which is suitable for surface treatment of 16Mn steel weld joint [9-15]. However, the structure of the single-layer coating is not uniform, and there are problems such as high porosity and unsatisfactory corrosion resistance that affect the durability. It can only provide physical shielding for the substrate and inhibit corrosion by blocking the penetration of corrosive media. It is found that duplex coating can greatly protect the substrate during the corrosion. Due to the irregular arrangement of the unit cells of the inner and outer layer of the duplex layer coating, dislocations increase and the surface density can be effectively improved [16-20]. In addition, there is a certain potential difference between each layer of the coating, which changes the corrosion mechanism of the duplex coating. It is found out the nickel based coating possesses excellent chemical and physical properties [21-25]. In this study, a 16Mn steel plate is selected as the base metal for welding, and a Ni-P/Ni-Mo-P duplex coating with Ni-P coating as the inner layer and Ni-Mo-P coating as the outer layer is constructed on the surface of the weld joint by electroless plating. The appearance, surface morphology and composition of the weld joint with and without Ni-P/Ni-Mo-P duplex coating were analyzed, and the corrosion resistance of the weld joint with and without Ni-P/Ni-Mo-P duplex coating in natural seawater was also studied.

2. EXPERIMENTAL

2.1 Materials and reagents

A 16Mn steel plate with a size of 60 mm × 40 mm × 3 mm was selected as the base metal for welding. The weld joint structure is shown in Figure 1. The 16Mn steel was cut along the weld area as the substrate. After that, the sandpaper of grade 400#, 1200# and 2000# were used to grind the substrate of the sample step by step to make the surface bright. Subsequently, acetone and hot alkali solution (sodium hydroxide 15 g/L + sodium carbonate 40 g/L, 60 ℃) and dilute hydrochloric acid (mass concentration 10%, 30 ℃) were used to do the pretreatment for the substrate sequentially. Finally, the substrate was cleaned and dried to do the electroless plating.

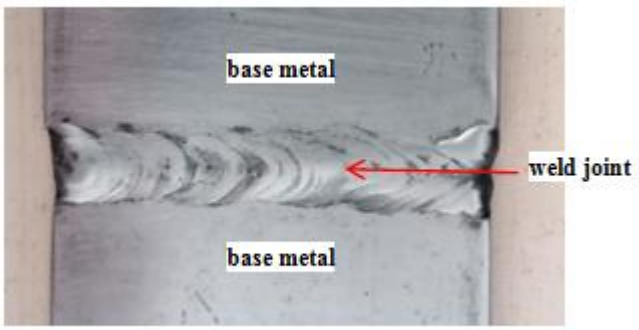

Figure 1. Weld joint structure of 16Mn steel

2.2 Electroless plating of Ni-P/Ni-Mo-P duplex coating

A Ni-P/Ni-Mo-P duplex coating with Ni-P coating as the inner layer and Ni-Mo-P coating as the outer layer was prepared on the surface of 16Mn steel substrate by electroless plating. The specific experimental procedure was as follows: a 16Mn steel substrate was firstly immersed into Ni-P electroless plating solution to do Ni-P electroless plating for 30 min. After that, the sample is rapidly immersed into the Ni-Mo-P electroless plating solution to do Ni-Mo-P electroless plating for 60 min. In addition, Ni-P single-layer coating and Ni-Mo-P single-layer coating were prepared respectively by electroless plating for 90 min from the same Ni-P electroless plating solution and Ni-Mo-P electroless plating solution. The bath composition and parameters were shown in Table 1.

Table 1. Bath composition and process parameters

Bath composition and process parameters	**Ni-P**	**Ni-Mo-P**
$NiSO_4 \cdot 6H_2O$/ ($g \cdot L^{-1}$)	20	25
$Na_2MoO_4 \cdot 2H_2O$ / ($g \cdot L^{-1}$)	—	2
$NaH_2PO_2 \cdot 2H_2O$ / ($g \cdot L^{-1}$)	22	11
$C_6H_5Na_3O_7 \cdot 2H_2O$ / ($g \cdot L^{-1}$)	10	32
$(NH_4)_2SO_4$ / ($g \cdot L^{-1}$)	36	36
$C_{12}H_{25}NaO_4S$ / ($mg \cdot L^{-1}$)	40	40
$C_3H_6O_3$ / ($g \cdot L^{-1}$)	—	9
pH	8.8~9.0	8.8~9.0
Temperature /°C	84±0.5	92±0.5

2.3 Testing

2.3.1 Surface morphology and composition

DSC-H300 optical camera and Nova NanoSEM450 scanning electron microscope were used to observe the appearance and surface morphology of substrate and different coatings before and after corrosion. The testing parameter of scanning electron microscope was set as 15 kV with 10 mm working distance. The composition of the substrate and different coatings were analyzed with the energy dispersive spectrometer attached to the scanning electron microscope with 10 kV accelerating voltage of surface sweep model.

In addition, the porosity of different coatings was tested by the filter paper method. First, put the filter paper in a solution made up of 15 g/L potassium ferricyanide and 25 g/L sodium chloride for 5 min. Subsequently, the filter paper was taken out and put it on the surface of different coatings. Finally, the number of spots per unit area on the filter paper was counted to calculate the porosity of different coatings.

2.3.2 Corrosion testing

The corrosion resistance of 16Mn steel substrate and different coatings were tested by putting the sample into natural seawater (salinity 3.2%) for 192 h at temperature 25 ℃. After the experiment, it was dried and weighed with an AB-204S electronic balance of 0.0001 g precision. The mass loss and corrosion rate of the substrate and different coatings were calculated. Parstat2273 electrochemical workstation was used to test the polarization curves of different coatings in natural seawater. Saturated calomel electrode and platinum plate were used as reference electrode and auxiliary electrode, respectively. The scan rate was set to 1 mV/s. The test results were fitted with the PowerSuite software that comes with the electrochemical workstation, and the corrosion potential, corrosion current density and the protection efficiency of different coatings were obtained.

3. RESULTS AND DISCUSSION

3.1 Surface morphology and composition

Figure 2 shows the appearance and surface morphology of the substrate and different coatings. The comparison shows that the Ni-P single-layer coating, Ni-Mo-P single-layer coating and Ni-P/Ni-Mo-P duplex coating all cover the weld joint completely showing a nodular morphology.

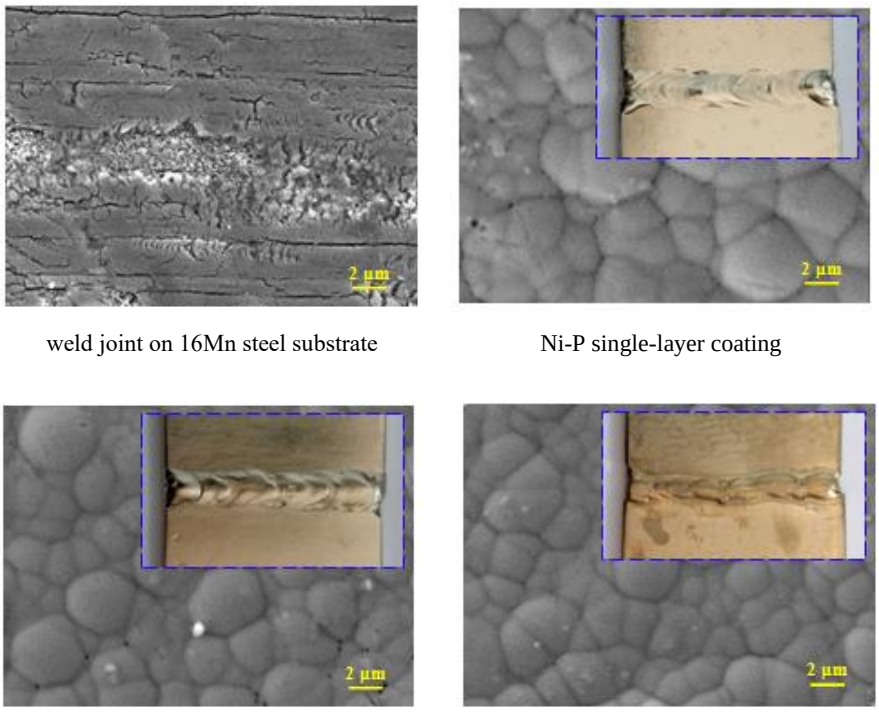

weld joint on 16Mn steel substrate | Ni-P single-layer coating

Ni-Mo-P single-layer coating | Ni-P/Ni-Mo-P duplex coating

Figure 2. Appearance and surface morphology of the substrate and different coatings; Accelerating voltage is 15 kV with work distance 10 mm;

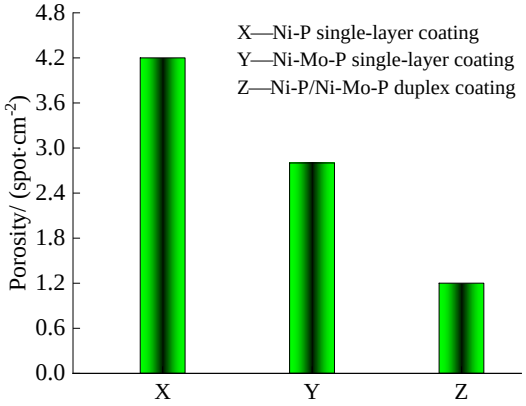

Figure 3. Porosity of differnt coatings

The nodular morphology of alloy coatings has been described by several researchers [26-28]. Some people also prepared Ni-P coatings of amorphous structure which may be due to different amounts of phosphorus in the coating [29-31]. However, the surfaces of Ni-P single-layer coating and Ni-Mo-P single-layer coating are porous. The porosity is 4.2 spot/cm^2 and 2.8 spot/cm^2, as shown in Figure 3. However, the Ni-P/Ni-Mo-P duplex coating has almost no pores, and its porosity is only 1.2 spot/cm^2. This is due to the irregular arrangement of the unit cells of the inner Ni-P coating and the outer Ni-Mo-P coating, which increases dislocations and reduces the porosity. Therefore, its surface density is better than that of the Ni-P single-layer coating and Ni-Mo-P single-layer coating.

According to the data in Figure 4, the composition of the 16Mn steel substrate is Fe, C and Cr elements, with Fe as the main element. The composition of Ni-P single-layer coating is Ni and P elements, with Ni as the main element. The composition of Ni-Mo-P single-layer coating is Ni, Mo and P elements. The composition of Ni-P/Ni-Mo-P duplex coating is also Ni, P and Mo elements, and the content of Ni element is the highest.

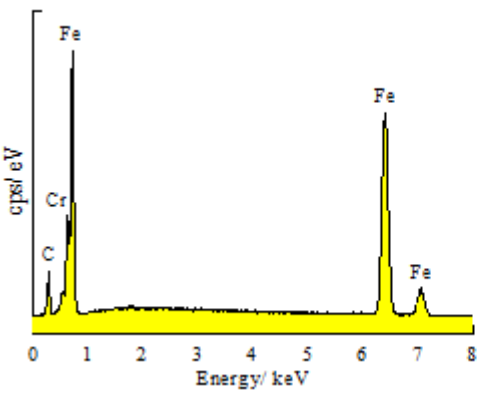

16Mn steel substrate

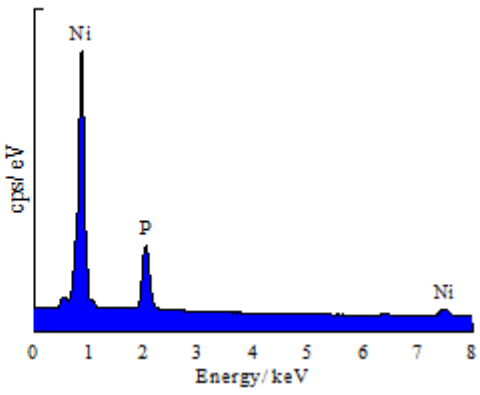

Ni-P single-layer coating

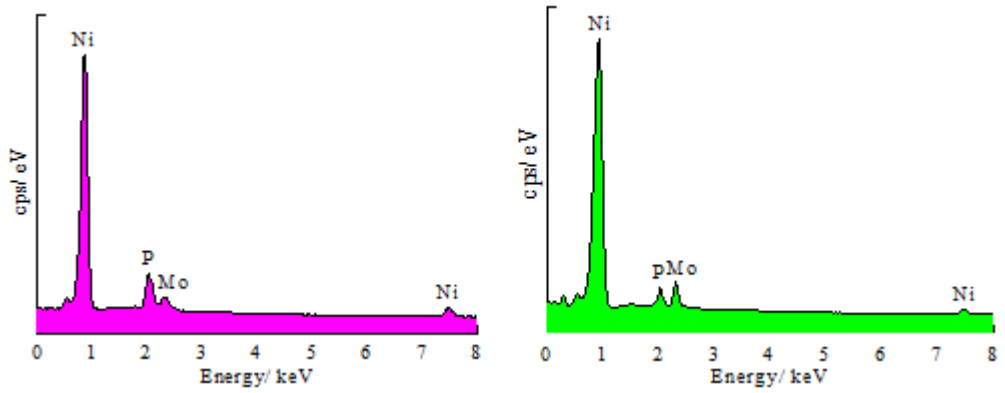

Ni-Mo-P single-layer coating Ni-P/Ni-Mo-P duplex coating

Figure 4. Energy spectra of the substrate and different coatings; Accelerating voltage is 10 kV with surface sweep model;

3.2 Corrosion rate and morphology of 16Mn steel substrate and different coatings

Figure 5 shows the variation trend of the corrosion rate of the substrate and different coatings immersion in natural seawater for different times. It can be seen from Figure 5 that after immersion in natural seawater for 24 h, the corrosion rate of the substrate, Ni-P single-layer coating, Ni-Mo-P single-layer coating and Ni-P/Ni-Mo-P duplex coating all start to increase. After immersion in natural seawater for 72 h, the corrosion rate of the substrate, Ni-P single-layer coating, Ni-Mo-P single-layer coating and Ni-P/Ni-Mo-P duplex coating shows differences. Meanwhile, the corrosion rate of the Ni-P/Ni-Mo-P duplex coating is the lowest. After immersion in natural seawater for 120 h, the corrosion rate of the substrate continues to increase, but the slope of the corrosion rate for Ni-P single-layer coating, Ni-Mo-P single-layer coating and Ni-P/Ni-Mo-P duplex coating decreases gradually which indicates that the single-layer coating or duplex coating is beneficial to increase the corrosion resistance of substrate.

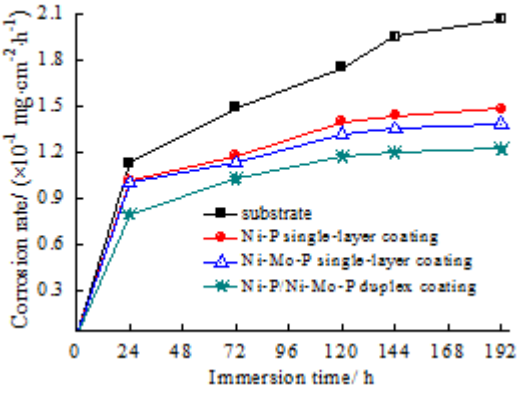

Figure 5. Variation trend of corrosion rate of the substrate and different coatings immersion in natural seawater for different times at 25 ℃

According to the analysis, the mass loss of Ni-P single-layer coating, Ni-Mo-P single-layer coating and Ni-P/Ni-Mo-P duplex coating have no obvious change in the initial stage of corrosion, which means that they can better prevent the erosion of corrosive media in natural seawater. With the prolonging of immersion time in natural seawater, the coating was gradually destroyed due to the synergistic effect of oxygen atoms and chloride ions, which shows an increase in the corrosion rate. However, with the increase of products generated during the corrosion process accumulated and filled on the corrosion pit and the surface of the coating can prevent the continued adsorption and further diffusion of oxygen atoms and chloride ions, so the corrosion rate increases slowly and then tends to be stable [32-33]. During the corrosion cycle, the corrosion rate of the Ni-P/Ni-Mo-P duplex coating is lower than that of the Ni-P single-layer coating and Ni-Mo-P single-layer coating, indicating that its corrosion resistance is better. Compared with single-layer coating, duplex coating generally has better corrosion resistance, which has been reported in many literatures [34-37].

Figure 6 shows the corrosion morphology of the substrate and different coatings after immersion in natural seawater for 192 h. It can be seen from Figure 6(a) that the corrosion degree of the substrate is very serious. Most of the surface is broken and longer and deep cracks are formed. It can be seen from Figure 6(b), Figure 6(c) and Figure 6(d) that the corrosion degree of Ni-P single-layer coating, Ni-Mo-P single-layer coating and Ni-P/Ni-Mo-P duplex coating are all significantly lighter than that of the substrate.

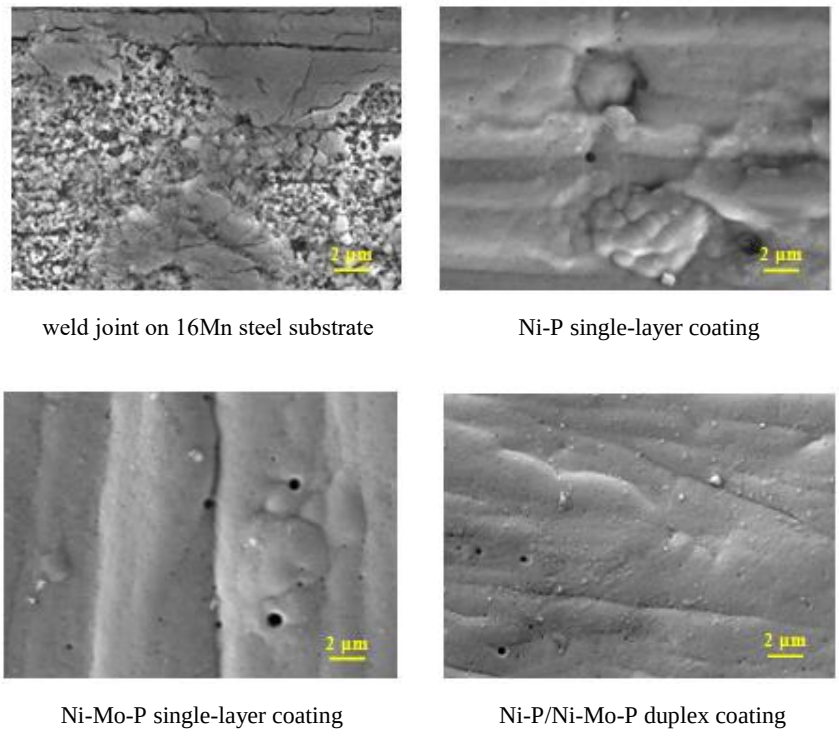

Figure 6. Corrosion morphology of the substrate and different coatings after immersion in natural seawater for 192 h at 25 ℃

There is no cracking phenomenon caused by corrosion, but the porosity of their surfaces

increase considerably and their diameters become larger than those before testing. Among them, the Ni-P/Ni-Mo-P duplex coating has the lightest corrosion degree, and the pores formed on the surface have a small diameter, which confirms that its barrier effect on the diffusion and penetration of the corrosive medium is stronger.

3.3. Polarization curves of substrate and different coatings

Figure 7 shows the polarization curves of the substrate and different coatings in natural seawater. It can be seen from Figure 8 that the order of corrosion potential from negative to positive is as follows: substrate, Ni-P single-layer coating, Ni-Mo-P single-layer coating, Ni-P/Ni-Mo-P duplex coating. The order of corrosion current density from low to high is as follows: Ni-P/Ni-Mo-P duplex coating, Ni-Mo-P single-layer coating, Ni-P single-layer coating, substrate. The corrosion resistance of Ni-P single-layer coating and Ni-Mo-P single-layer coating are also investigated by some researchers [39-40]. Ni-P/Ni-Mo-P duplex coating has the most positive corrosion potential and the minimum corrosion current density. Compared with the substrate, the corrosion potential of Ni-P/Ni-Mo-P duplex coating shifts about 155 mV to more positive position. Moreover, the corrosion current density of Ni-P/Ni-Mo-P duplex coating is the lowest indicating best corrosion resistance which can better reduce the corrosion tendency and inhibit the development of corrosion. The reason is that there is a certain potential difference between Ni-Mo-P coating and Ni-P coating. The corrosion mechanism of Ni-P/Ni-Mo-P duplex coating is different from that of Ni-P single-layer coating and Ni-Mo-P single-layer coating. In addition, the Ni-P /Ni-Mo-P duplex coating has low porosity and good surface density, which effectively prevents the corrosive medium from penetrating into the coating through holes as channels, thus inhibiting the development of corrosion and showing better corrosion resistance. The corrosion mechanism of Ni-P single-layer coating and duplex coating is investigated by Wang [41].

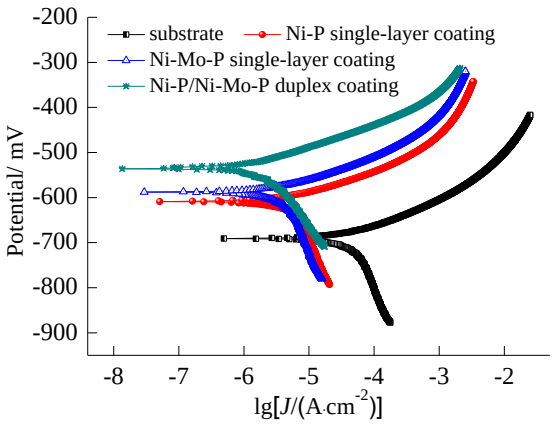

Figure 7. Polarization curves of the substrate and different coatings in natural seawater

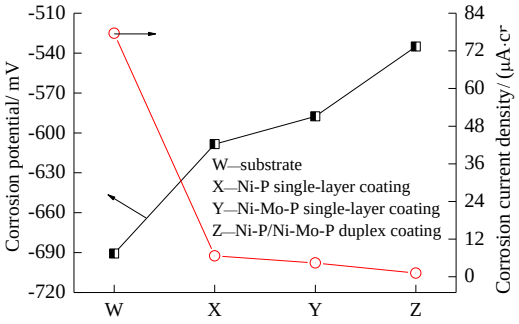

Figure 8. Corrosion potential and corrosion current density of the substrate and different coatings

Figure 9 shows the protection efficiency of different coatings on the substrate. It shows that Ni-P/Ni-Mo-P duplex coating has the highest protection efficiency, reaching 98.5%, which is significantly higher than that of Ni-P single-layer coating and Ni-Mo-P single-layer coating. The study shows that the higher the protection efficiency, the better the corrosion resistance of the coating. Compared with Ni-P single-layer coating and Ni-Mo-P single-layer coating, Ni-P/Ni-Mo-P duplex coating has lower porosity and better surface density, which prolongs the penetration path of the corrosive medium and effectively prevents its contact with the substrate, thus slowing down the corrosion. Therefore, Ni-P/Ni-Mo-P layer coating can better protect the substrate and significantly improve the corrosion resistance in natural seawater.

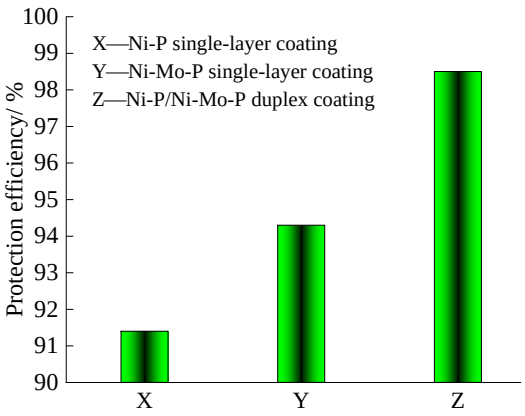

Figure 9. Protection efficiency of different coatings

4. CONCLUSIONS

(1) A Ni-P/Ni-Mo-P duplex coating with Ni-P coating as the inner layer and Ni-Mo-P coating as the outer layer was constructed on the surface of 16Mn steel by electroless plating. The porosity of the duplex coating was only 1.2 spot/cm^2 corresponding to the lowest corrosion rate and the lightest corrosion degree. The corrosion current density of the duplex coating is nearly two orders of magnitude lower than that of the substrate, with a 98.5% protection efficiency, thus playing a

significant role in corrosion protection and significantly improve the corrosion resistance in natural seawater.

(2) The composition of Ni-P/Ni-Mo-P duplex coating is Ni, P and Mo elements, as in the case of the Ni-Mo-P single-layer coating. Compared with Ni-P single-layer coating and Ni-Mo-P single-layer coating, the duplex coating has better surface densification, lower corrosion rate and corrosion current density with higher protection efficiency. There is a certain potential difference between the Ni-Mo-P coating and Ni-P coating, so that the corrosion mechanism of Ni-P/Ni-Mo-P duplex coating is different from that of Ni-P single-layer coating and Ni-Mo-P single-layer coating.

References

1. R. Cao, C. Han, X. L. Guo, Y. Jiang, F. Liao, G. S. Dou, Y. J. Yan and J. H. Chen, *Mater. Sci. Eng., A*, 833 (2022) 142560.
2. T. Y. Zhang, W. Liu, B. J. Dong, Y. J. Wu, W. J. Yang, Y. G. Zhao, Y. M. Fan and L. J. Chen, *Mater. Chem. Phys.*, 276 (2022) 125365.
3. Y. H. Sun and Y. F. Cheng, *Eng. Fail. Anal.*, 133 (2022) 105985.
4. Q. Wang, X. M. Cao, T. Q. Wu, M. Liu, C. Li and F. C. Yin, *Int. J. Press. Vessels Pip.*, 194 (2021) 104508.
5. Y. Yang, X. Zhang, Z. He, J. L. Guo and Y. Liu, *Ocean Eng.*, 235 (2021) 109370.
6. Y. Q. Huang, J. K. Huang, J. X. Zhang, X. Q. Yu, Q. Li, Z. Wang and D. Fan, *Mater. Today Commun.*, 29 (2021) 102948.
7. Y. W. Xu, X. Q. Hou, Y. Shi, W. Z. Zhang, Y. F. Gu, C. G. Feng and K. Volodymyr, *Corros. Sci.*, 191 (2021) 109729.
8. M. L. Cheng, P. He, L. L. Lei, X. Tan, X. Y. Wang, Y. T. Sun, J. Li and Y. M. Jiang, *Corros. Sci.*, 183 (2021) 109338.9. Y. D. Yu, M. G. Li, G. Y. Wei and H. L. Ge, Surf. Eng., 29 (2013) 767.
9. Y. D. Yu, M. G. Li, G. Y. Wei and H. L. Ge, *Surf. Eng.*, 29 (2013) 767.
10. A. Solimani, T. M. Meibner, C. Oskay and M. C. Galetz, *Sol. Energy Mater. Sol. Cells*, 231 (2021) 111312.
11. V. Nemane and S. Chatterjee, *Mater. Charact.*, 180 (2021) 111414.
12. V. Vitry, J. Hastir, A. megret, S. Yazdani, M. Yunacti and L. Bonin, *Surf. Coat. Technol.*, 429 (2022) 127937.
13. Y. D. Yu, Z. L. Song, H. L. Ge and G. Y. Wei, *Prog. Nat. Sci.: Mater. Int.*, 24 (2014) 232.
14. G. X. Dai, S. P. Wu and X. X. Huang, *J. Alloys Compd.*, 902 (2022) 163736.
15. J. T. Wang, X. L. Bai, X. H. Shen, X. F. Liu and B. L. Wang, *J. Manuf. Processes*, 74 (2022) 296.
16. J. Zhang, Z. H. Xie, H. Chen, C. Hu, L. X. Li, B. N. Hu, Z. W. Song, D. L. Yan and G. Yu, *Surf. Coat. Technol.*, 342 (2018) 178.
17. Q. Y. Wang, Y. C. Xi, J. Xu, S. Liu, Y. H. Lin, Y. H. Zhao and S. L. Bai, *J. Alloys Compd.*, 729 (2017) 787.
18. Q. Zheng, F. Dierre, V. Corregidor, R. Fernandez-Ruiz, J. Crocco, H. Bensalah, E. Alves and E. Dieguez, *J. Cryst. Growth*, 358 (2012) 89.
19. A. S. Dominguez, J. J. P. Bueno, I. Z. Torres and M. L. M. Lopez, *Surf. Coat. Technol.*, 326 (2017) 192.
20. J. A. Liu, S. H. Li, Z. W. Han and R. Z. Cao, *Mater. Chem. Phys.*, 257 (2021) 123753.
21. Y. H. Hu, Y. D. Yu, H. L. Ge, G. Y. Wei and L. Jiang, *Int. J. Electrochem. Sci*., 14 (2019) 1649.
22. A. Lelevic and F. C. Walsh, *Surf. Coat. Technol.*, 369 (2019) 198.
23. V. B. Llorente, L. A. Diaz, G. I. Lacconi, G. C. Abuin and E. A. Franceschini, *J. Alloys Compd.*, 897 (2022) 163161.

24. V. V. Kuznetsov, Y. D. Gamburg, V. V. Zhulikov, V. M. Krutskikh, E. A. Filatova, A. L. Trigub and O. A. Belyakova, *Electrochim. Acta*, 354 (2020) 136610.
25. D. Figuet, A. Billard, C. Savall, J. Creus, S. Cohendoz and J. L. Grosseau-Poussard, *Mater. Chem. Phys.*, 276 (2022) 125332.
26. H. Algul, M. Uysal and A. Alp, *Appl. Surf. Sci. Adv.*, 4 (2021) 100089.
27. Y. D. Yu, G. Y. Wei, L. Jiang and H. L. Ge, *Int. J. Electrochem. Sci.*, 15 (2020) 1108.
28. W. J. Yuan, Z. D. Cui, S. L. Zhu, Z. Y. Li, S. L. Wu and Y. Q. Liang, *Electrochim. Acta*, 365 (2021) 137366.
29. S. Samanta, K. Mondal, M. Dutta and S. B. Singh, *Surf. Coat. Technol.*, 409 (2021) 126928.
30. A. Szasz, J. Kojnok, L. Kertesz and Z. Hegedus, *J. Non-Cryst. Solids*, 57 (1983) 213.
31. Y. C. Wu, K. Xu, Z. Y. Zhang, X. R. Dai, S. Yang, H. Zhu, J. Gao and Y. Liu, *Surf. Coat. Technol.*, 429 (2022) 127961.
32. A. Comer and L. Looney, *Int. J. Fatigue*, 28 (2006) 826.
33. V. Kramar, V. Dushko, A. Rodkina and A. Zaiets, *Procedia Eng.*, 100 (2015) 1068.
34. H. Kovaci, Y. B. Bozkurt, A. F. Yetim, O. Baran and A. Celik, *Tribol. Int.*, 156 (2021) 106823.
35. Y. Q. Rao, Q. Wang, J. X. Chen and C. S. Ramachandran, *Mater. Today Commun.*, 26 (2021) 101978.
36. S. Rahmani, A. Omrani and S. Shabanpanah, *Surf. Coat. Technol.*, 373 (2019) 1.
37. M. R. S. Beyragh, S. K. Asl and S. Norouzi, *Surf. Coat. Technol.*, 205 (2010) 2605.
38. A. Salicio-Paz, H. Grande, E. Pellicer, J. Sort, J. Fornell, R. Offoiach, M. Lekka and E. Garcia-Lecina, *Surf. Coat. Technol.*, 368 (2019) 138.
39. J. Wojewoda-Budka, A. Wierzbicka-Miernik, I. Kwiecien, F. Valenza, A. Korneva, M. Janusz-Skuza, K. Stan-Glowinska, J. Guspiel and M. Bugajska, *Electrochim. Acta*, 406 (2022) 139850.
40. M. E. Mert, B. D. Mert, G. Kardas and B. Yazici, *Appl. Surf. Sci.*, 423 (2017) 704.
41. Y. X. Wang, X. Shu, S. H. Wei, C. M. Liu, W. Gao, R. A. Shakoor and R. Kahraman, *J. Alloys Compd.*, 630 (2015) 189.